Research Article

Rapid Communications in Mass Spectrometry

Received: 30 June 2016 Revised: 19 September 2016 Accepted: 5 October 2016 Published online in Wiley Online Library

Rapid Commun. Mass Spectrom. **2016**, *30*, 2655–2663
(wileyonlinelibrary.com) DOI: 10.1002/rcm.7762

Chromatographic peak reconstruction algorithm to improve qualitative and quantitative analysis of trace pesticide residues

Xiu-Ping Chen[1,2], Ruo-Jing Fan[2], Fang Zhang[2]*, Zhong-Quan Li[2], Bin Xu[1] and Yin-Long Guo[2]**

[1]Department of Chemistry, Innovative Drug Research Center, Shanghai University, 99 Shangda Road, Shanghai 200444, China
[2]State Key Laboratory of Organometallic Chemistry and National Center for Organic Mass Spectrometry in Shanghai, Shanghai Institute of Organic Chemistry, Chinese Academy of Sciences, 345 Lingling Road, Shanghai 200032, China

RATIONALE: In order to improve analysis of analytes in trace amounts in a complex matrix, we developed a novel post-processing method, named Chromatographic Peak Reconstruction (CPR), to process the recorded data from gas chromatography/time-of-flight mass spectrometry (GC/TOFMS).
METHODS: For a trace ion, the relative deviation (δ) between the adjacent scanned mass-to-charge ratios (m/z) was found to be inversely proportional to its MS peak intensity. Based on this relationship, the thresholds of δ value within the specified intensity segments were estimated by the CPR and used to screen out the suspicious scan-points in the extracted ion chromatographic (EIC) peak. Then, the intensities of these suspicious scan-points were calibrated to reconstruct a new EIC peak.
RESULTS: In the qualitative analysis of 118 pesticides, 107 out of the test pesticides can be confirmed. The corrected response ratios of the qualitative ion (q) over the quantitative ion (Q), q/Q, became closer to their references. In the quantitative analysis of 10 test pesticides at 5 ppb, the relative errors of the calculated concentrations after using the CPR were below ±1.55%, down from ±2.29% without using the CPR.
CONCLUSIONS: The developed CPR showed great potential in the analysis of trace analytes in complex matrices. It was proved to be a helpful data processing method for the monitoring of trace pesticide residues. Copyright © 2016 John Wiley & Sons, Ltd.

As one of the important symbols of human civilization, wide applications of pesticides have made a noticeable contribution to modern agriculture by improving economic outputs. However, such wide uses and sometime abuses have caused environmental pollution and left residues in the applied subjects. Pesticide residues left in food and water impose a potential threat to the health of human and animals,[1–5] even after the applied pesticides are thought to have dissipated completely.[6] In order to prevent pesticide residue-induced diseases and ensure food chain safety, a nationwide program have presently been established to monitor pesticide residues in food and drinking water.[7–10] Methods featured with higher accuracy, resolution and detection sensitivity are being explored for the monitoring of pesticide residues, especially severely restricted pesticides in trace amounts.[11–13]

* *Correspondence to:* F. Zhang, State Key Laboratory of Organometallic Chemistry and National Center for Organic Mass Spectrometry in Shanghai, Shanghai Institute of Organic Chemistry, Chinese Academy of Sciences, 345 Lingling Road, Shanghai 200032, China.
E-mail: fzhang@sioc.ac.cn
** *Correspondence to:* B. Xu, Department of Chemistry, Innovative Drug Research Center, Shanghai University, 99 Shangda Road, Shanghai 200444, China.
E-mail: xubin@shu.edu.cn

To date, gas chromatography/time-of-flight mass spectrometry (GC/TOFMS) is a powerful technique for volatile and semi-volatile pesticide analyses due to the remarkable separation power of the GC and the higher resolution of the TOFMS.[14–16] TOFMS can provide the high mass accuracy of full-scan spectra at a fast scan rate,[17–20] even for pesticides at the trace level in a complex matrix. However, identifying all of the underlying signals in a complex sample remains challenging as the signals of interest may be obscured by interfering signals.[21,22] These interfering signals, mainly originating from random noise and background ions,[23–26] complicate the data analysis. Hence, methods of eliminating any signals not related to analytes become important.

Background subtraction algorithms,[27–29] which are used to reduce background ion signals and random noise, have been explored for many years. They subtract undesired signals from the data of a sample to avoid false indications of the presence of components or compounds.[30,31] Recently, other types of algorithms used to obtain 'clean' signals of analytes have been developed. For example, Wang *et al*. employed an ion trace detection algorithm based on the relative mass difference tolerance to extract pure ion chromatograms.[32] Adutwum *et al*. developed a data reduction tool termed 'unique ion filter' to remove variables that are likely unimportant or redundant in a chromatographic sense.[33] However, if the parameters are not set appropriately, the algorithms in the play of their functions may also remove useful signals, select false signals,

or generate split peaks, further complicating the subsequent data analysis.[34] Furthermore, removing the interfering signals or picking out the true signals directly is not sufficient for the accurate detection of analytes presenting at trace level in complex samples. The peaks of the analytes in the mass spectra may be convoluted by interfering signals, which change the mass-to-charge ratios (*m/z*) and the intensities of mass spectra peaks (MS peaks).[35] The deviant intensities of MS peaks may form deviant chromatographic peaks for the analytes, which increase the difficulty of accurate qualification and quantitation. Thus, eliminating the impact of interfering signals on the true signals is also necessary.

To eliminate interfering signals and reduce their impact on true signals, thereby enabling more accurate qualification and quantitation, we developed a novel post-processing method for data from a high-resolution MS instrument, the Chromatographic Peak Reconstruction (CPR) method, to analyze trace ions in complex matrices. The relative deviations between adjacent scanned target *m/z* values were calculated. Then, the estimated thresholds of relative deviations were used to screen out the suspicious scan-points in the extracted ion chromatographic (EIC) peak of the target ion. Finally, the intensities of suspicious scan-points were calibrated to reconstruct a new EIC peak. To evaluate the applicability of the CPR algorithm, a series of vegetable and fruit samples spiked with pesticides were detected using GC/TOFMS. The recorded data were processed using the CPR method and the reconstructed EIC peaks were used for qualitative and quantitative analyses.

EXPERIMENTAL

Materials

Bond Elut Carbon/NH_2 cartridges (500 mg/500 mg, 6 mL) were supplied by Agilent Technologies (Santa Clara, CA, USA). A total of 118 pesticides were obtained from J&K Scientific Ltd (Beijing, PR China). n-Hexane (HPLC grade) was supplied by Fisher Scientific (Santa Clara, CA, USA). Other solvents and reagents (analytical grade purity) were purchased from Shanghai Reagent Company (Shanghai, PR China). The fresh organic apple, scallion and spinach were supplied by a local market (Shanghai, PR China).

Sample preparation

The fresh apple, scallion and spinach were chopped into small pieces, respectively. Each 20 g of the chopped matrix was mixed with 40 mL acetonitrile in an 80-mL centrifugal tube. Then the mixture was blended at 15,000 rpm (1 min). During the blending, 5 g of sodium chloride was added. The sample homogenate was centrifuged at 4200 rpm (5 min). For further clean-up, the supernatant (20 mL) was transferred into a 100-mL rotary evaporator flask and concentrated to 1 mL at 40°C.

The Bond Elut Carbon/NH_2 cartridge (500 mg/500 mg, 6 mL) with 2 cm anhydrous sodium sulfate added was activated by 4 mL of acetonitrile/toluene (3:1). After that, the extract solution (1 mL) was applied to the cartridge followed by the elution with 25 mL of acetonitrile/toluene (3:1). The entire volume of effluent was collected and concentrated to 0.5 mL by rotary evaporation at 40°C. The residue was dissolved in n-hexane to make a 10 mL blank matrix solution for detection.

A standard mixture solution of the 118 pesticides was prepared at a concentration of 5 ppm in n-hexane to fortify the spiked samples. Four concentrations of the matrix spiked pesticides are 1, 2, 5 and 10 ppb, and they were prepared by a proper dilution of the standard solution in the blank matrix solution.

Instrument and software

A 7200 accurate-mass GC/QTOFMS instrument (Agilent Technologies, Santa Clara, CA, USA) with a fused-silica DB-35 MS capillary column (30 m × 0.25 mm i.d.) was used for the determination of pesticide residues. The GC oven temperature was programmed starting at 80°C held for 1 min, followed by increase of 25°C/min to 170°C, and at 6°C /min to a final temperature of 300°C and held for 10 min. Splitless injections of 1 μL sample were carried out at 250°C. Helium (purity >99.999%) was used as the carrier gas at a flow rate of 1.2 mL/min. The transfer line and ion source temperatures were set to 300°C and 250°C. TOF for MS was operated at an acquisition rate of 5spectra/s with the mass range of *m/z* 50–600. The resolution of the TOFMS was about 13,500 (full width at half maximum, FWHM). Perfluorotributylamine (PFTBA) was used for daily mass calibration.

MassHunter Qualitative Analysis B.06.00 (Agilent Technologies, Santa Clara, CA, USA), IBM SPSS Statistics version 21 (IBM Corporation, Armonk, NY, USA) and Origin 8 SR0 v8.0725 (B725) (OriginLab Corp., Northampton, MA, USA) were used for the treatment of data. A self-built pesticide library[6,15] was used for the determination.

CPR algorithm

There are five steps in the CPR algorithm, as shown in Supplementary Fig. S1 (Supporting Information).

Step 1: Obtain target chromatographic peaks by extracting ion chromatograms. The high mass resolution of TOFMS enables the recording of extracted ion chromatograms with a narrow mass window, allowing it to effectively subtract the interfering signals while retaining the true signals. In this study, the mass window was optimized to a width of ±10 mDa according to the QTOFMS used, which ensures that the obtained signals correspond to a single ion in each extraction.

Step 2: Create scan-sorted MS peak tables based on the EIC peaks. For each target ion, the recorded *m/z* values and their intensities in the consecutive mass spectra scans are exported to an *Excel* file. These data are sorted by the scan number to generate a scan-sorted MS peak table. Each target ion has its own table.

Step 3: Calculate the relative deviations (δ) between adjacent *m/z* values collected in the scan-sorted MS peak tables using Eqn. (1):

$$\delta = \frac{|m_k - m_{k+1}|}{m_k} \times 10^6 \quad (1)$$

where m_k and m_{k+1} are the recorded *m/z* values at the *k*th and *k* + 1th scan of the consecutive mass spectra. When the exact *m/z* value (m_{exact}) of the target ion is known, the δ value can be calculated with Eqn. (2):

Rapid Communications in Mass Spectrometry

$$\delta = \frac{|m_k - m_{k+1}|}{m_{exact}} \times 10^6 \quad (2)$$

Step 4: Estimate the thresholds (T_δ) of δ values within specified intensity segments. These T_δ values are used as the confidence limits for the screening of the suspicious scan-points. There are three critical processes:

(A) The MS peak intensities in tables are divided into several segments, such as >20,000 counts, 10,000–20,000 counts, 4000–10,000 counts, 2000–4000 counts, and <2000 counts.

(B) All δ values from all the tables are re-grouped based on these intensity segments. The δ values whose intensities are within the same intensity segment are grouped together.

(C) The confidence interval of the δ values belonging to the same segment is calculated at the 95% confidence level. The upper confidence limit is defined as the T_δ value of the specified intensity segment. The following are the concrete calculation formulas:The average ($\overline{\delta_j}$) of the δ values in the jth intensity segment is:

$$\overline{\delta_j} = \frac{1}{n}\sum_{i=1}^{n} \delta_{i,j} \quad (3)$$

where n is the number of δ values in the jth intensity segment and $\delta_{i,j}$ is the ith δ value in the jth intensity segment.The standard deviation (S) of the δ values is defined as:

$$S = \sqrt{\frac{1}{n-1}\sum_{i-1}^{n}\left(\delta_{i,j} - \overline{\delta_j}\right)^2} \quad (4)$$

When the confidence level is 95%, the calculation of the admissible error ($\Delta\delta$) is:

$$\Delta\delta = \frac{S}{\sqrt{n}} t_{0.05/2,(n-1)} \quad (5)$$

The upper confidence limit ($\overline{\delta_j} + \Delta\delta$) is calculated using Eqns. (3) and (5). Finally, the T_δ value of the δ values in the jth intensity segment is calculated as:

$$T_\delta = \overline{\delta_j} + \frac{S}{\sqrt{n}} t_{0.05/2,(n-1)} \quad (6)$$

Step 5: Reconstruct a new EIC peak for a target ion. The process includes:

(A) The scan-point with the highest intensity in the raw EIC peak is defined as the initial scan-point for the screening. The stop-points of the screening occur when their intensities below 500 counts or their signal-to-noise ratios (S/N) more than 3.

(B) The recorded m/z values in the raw EIC peak are screened in order from the initial scan-point outward. If the δ value of the adjacent scan-points exceeds the corresponding T_δ value, the scan-point owning the lower intensity will be identified as a suspicious scan-point.

(C) Based on the nearest reliable scan-points before and after the suspicious scan-point, a linear relationship between intensity and scan-number is generated. The intensity of the suspicious scan-point is then calibrated using this linearity. The calculated intensity takes the place of the raw intensity and is collected into the scan-sorted MS peak table.

(D) Based on the corrected table, a new EIC peak is reconstructed using Origin 8 software. The area of the new EIC peak is used as the qualifier and quantifier for qualitative and quantitative analyses.

RESULTS AND DISCUSSION

Relationship between relative deviation and MS peak intensity

Mass measurement accuracy can be affected not only by instrument mass drift, but also by factors such as the total ion current (TIC), the trapped ion population and the distribution of ion abundance during an on-line separation cycle. In our previous work, the mass error between the recorded m/z value and the m_{exact} of the ion indicated a rule of volatility and sustainability in each GC–MS cycle (see Supplementary Fig. S2, Supporting Information). The mass error and the MS peak intensity have been shown to be non-significantly correlated ($p > 0.1$). However, the discrete degree of the mass error became smaller with the increasing intensity and tended to reach stabilization (see Supplementary Fig. S3, Supporting Information). Considering that the volatility and sustainability of the mass error were generated under similar testing environments as the adjacent scan-points, this discovery inspired the question of whether the δ value between the adjacent scanned m/z values of the target ion has a relationship with the recorded m/z value or MS peak intensity of the ion. With this in mind, a standard solution spiked with multiple pesticides was analyzed by GC/QTOFMS. Eight pesticides, which were at a controlled concentration of 5 ppb and were known to be distributed throughout the GC/MS cycle (see Supplementary Fig. S4, Supporting Information), were selected for validation. The δ values of the eight representative ions were calculated using Eqn. (2).

The δ value was not correlated with the recorded m/z value (Fig. 1(A), $r = -0.016$, $p > 0.1$, $n = 181$). However, the δ value was negatively correlated with the intensity ($r = -0.334$, $p < 0.01$, $n = 181$) (Fig. 1(B)), especially when the intensity was below 20,000 counts (the δ value was relatively stable when the intensity was above 20,000 counts). The variability of the δ value clearly rose at a lower intensity since the impact of interfering signals on true signals increased. In Fig. 1(B), the variability showed a steep increase with a δ value up to 37.40 ppm for a signal intensity lower than 2000 counts. In contrast, the δ values were lower than 6.00 ppm for the intensities higher than 10,000 counts. Although some published studies have reported that the δ value is proportional to the corresponding intensity,[32] this relationship has an important assumption: the ions have high, even saturated abundance. In our investigation, this proportional relation was not suitable for use in the low-abundance range.

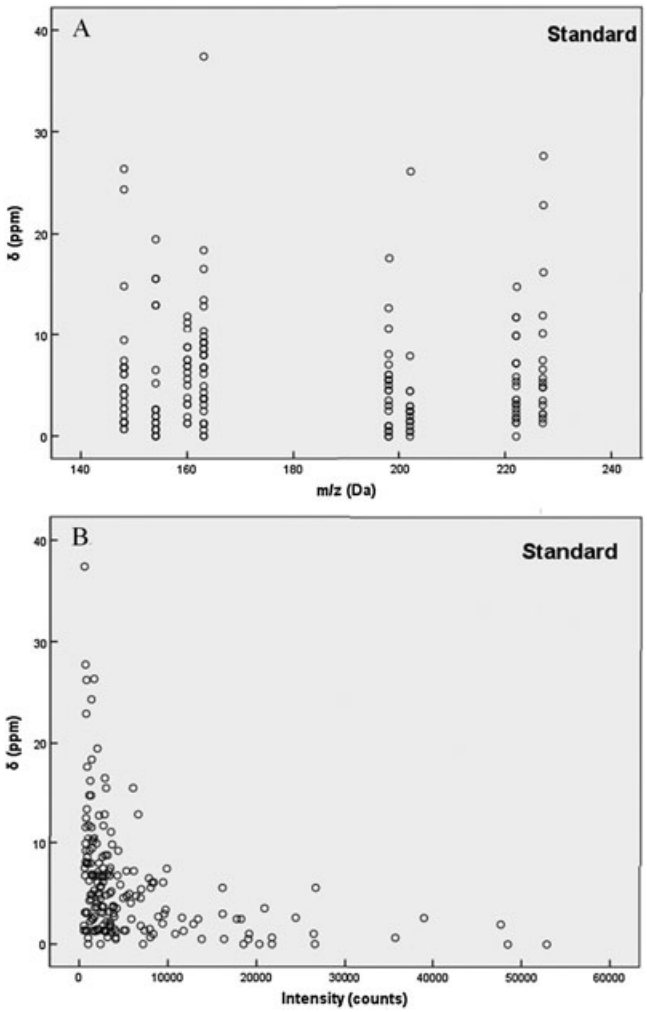

Figure 1. δ value was uncorrelated with recorded *m/z* value (A). However, δ value showed to be negatively correlated with MS peak intensity (B).

Moreover, to clarify the influence of different matrices, three matrix extracts from apple, scallion and spinach spiked with the same pesticides were analyzed. Similar results (see Supplementary Fig. S5, Supporting Information) also demonstrated a negative correlation. For an ion with low intensity (named trace ion), the δ value is negatively correlated with its MS peak intensity, no matter what the matrix is. Additionally, the matrix increases the interference on the trace ions, which is reflected in the variability of the δ value.

Estimation of thresholds for relative deviations

Based on our CPR algorithm, estimating the T_δ values for the δ values is a prerequisite for EIC peak reconstruction. As a model, each of the aforementioned eight ions, with their *m/z* values, δ values and intensities, were compiled into a table following the illustration in Steps 1–3 of "CPR Algorithm". Then, all the δ values from the eight tables are re-grouped based on the intensity segments, and the δ values within the same intensity segment are grouped together. The T_δ values were then estimated using the statistical calculations, and the results are shown in Fig. 2. For a standard sample, when the intensity was greater than 20,000 counts, the T_δ value of the δ values was as low as 2.47 ppm. Then, it increased as the intensity decreased. The other estimated T_δ values were 2.65 ppm (10,000–20,000 counts), 5.66 ppm (4000–10,000 counts), 6.24 ppm (2000–4000 counts), and 11.40 ppm (<2000 counts). It is worth mentioning that the scan-points with intensities below 500 counts or with S/N less than 3 were omitted when the interfering signals became relatively high and the true signals were hardly distinguished.

Among the standard solution and the three matrices, the T_δ values from the extract samples appeared to slightly deviate compared with the standard. One explanation is that the additional interference from the matrices might have affected the measurement stability. For example, the baselines of the EIC peaks for *p,p'*-methoxychlor and etofenprox clearly showed higher intensity in extract samples than in the standard sample. In addition, the additional interference from the different matrices also varied greatly. When the MS peak intensity increased and the influence of the interference diminished, the T_δ value decreased accordingly. The maximum T_δ value, 12.14 ppm, was from the spinach sample, in which the MS peak intensity was under 2000 counts. At the same level, the T_δ values of the apple and scallion samples were between 11.00 and 12.00 ppm. When the intensity was greater than 20,000 counts, the T_δ values of apple, scallion, and spinach were 2.05, 3.37, and 2.04 ppm, respectively. The δ values of the three matrix samples and the standard sample were tested by one-way analysis of variance (ANOVA), with p-values of 0.621, 0.281, 0.973, 0.017, and 0.915 when the intensity was above 20,000, between 10,000 and 20,000, between 4000 and 10,000, between 2000 and 4000, and under 2000 counts, respectively. Although a significant p-value of 0.017 ($p < 0.05$) was found for the intensity segment of 2000–4000 counts, the overall results did not show statistically significant differences. The results also indicated that the T_δ values were relatively constant and were less affected by the matrix. They could be used as reference values for screening suspicious scan-points in the EIC peaks.

Performance of reconstructed chromatographic peak

The reconstruction of the EIC peak is based on the generation of a corrected scan-sorted MS peak table. In general, the scan-point owning the highest intensity in the EIC peak is defined as the initial scan-point (red circles in Fig. 3) to start the screening. For example, for pyrimethanil, which is shown in Fig. 3(A), the 2346th scan-point was used as the initial scan-point. On the right side, the δ value between the 2346th and 2347th scan-points was compared with the corresponding T_δ value. If it did not exceed the T_δ value, the intensity of the 2347th scan-point would be kept and the δ value between the 2347th and 2348th scan-points would be compared in the same way. The left side of the screening began at the δ value between the 2346th and 2345th scan-points. In the process, if one δ value between the adjacent scan-points exceeded the corresponding T_δ value, the scan-point owning the lower intensity would be identified as the suspicious scan-point (the suspicious scan-points are shown in red in Fig. 3) and it would be

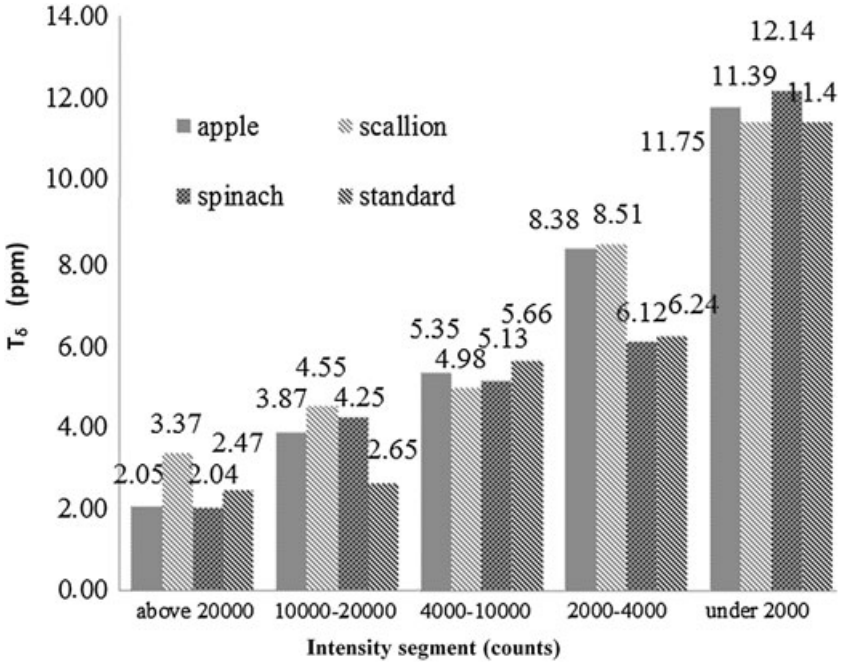

Figure 2. T_δ values of apple, scallion, spinach and standard samples.

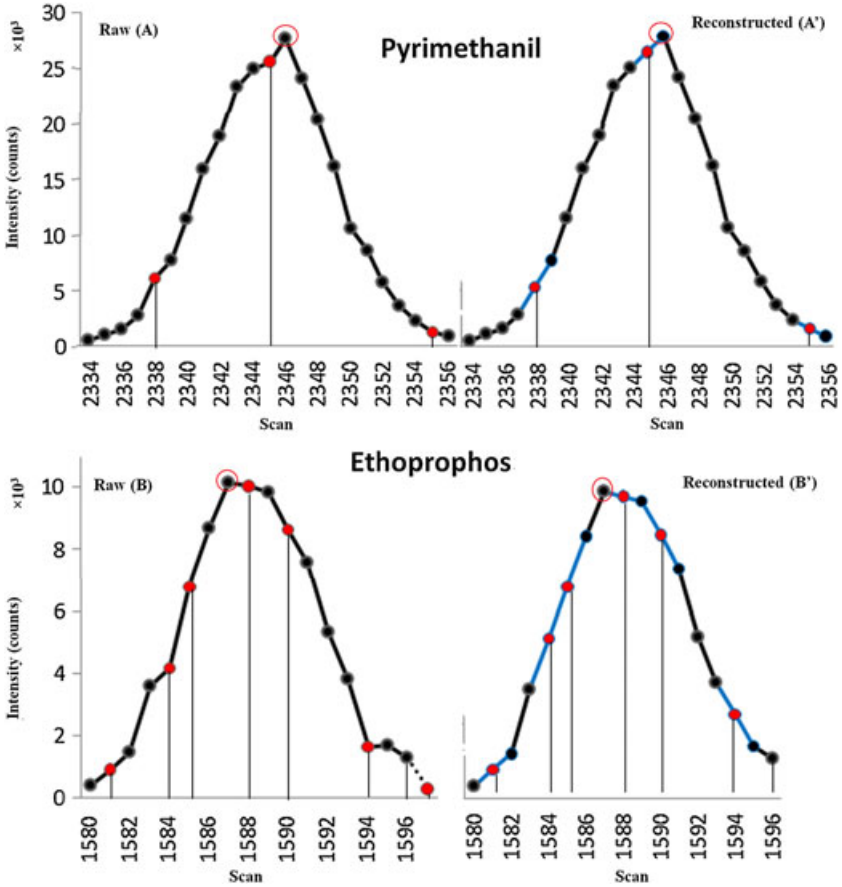

Figure 3. Raw (A, B) and reconstructed (A′, B′) EIC peaks of pyrimethanil and ethoprophos. The suspicious scan-points are red; the calibrated lines are blue; the initial scan-points are in red circles.

calibrated according to Step 5C in "CPR Algorithm". For example, the 2345th scan-point in Fig. 3(A) was suspicious. The δ value between the 2346th and 2345th scan-points was 3.53 ppm higher than the T_δ value of 2.05 ppm. From the blue line between the 2346th and 2344th scan-points, we could determine an intensity of 26343.34 counts for the 2345th scan-point (the calibration lines are in blue in Fig. 3). In the reconstruction, the calculated intensity as shown in Fig. 3(A′) took the place of the raw intensity. After screening out the suspicious 2345th scan-point, the recalculated δ value between the 2346th and 2344th scan-points was compared with the sum of the T_δ values of the 2345th and 2344th scan-points, for the screening of the 2344th scan-point. These comparisons were carried out until the scan-point possessed an intensity of less than 500 counts or until its S/N was less than 3. In the case of pyrimethanil, the stop-points on both sides were the 2334th and the 2356th scan-points.

In the CPR, two cases should be considered. First, if two or more suspicious scan-points are continuous, a linear relationship based on the closest reliable scan-points on either side of the suspicious scan-points is built to calibrate the intensities of the suspicious scan-points. For ethoprophos, whose raw EIC peak is shown in Fig. 3(B), the 1584th and 1585th scan-points were the suspicious scan-points. After screening out these suspicious scan-points, the recalculated δ value between the 1586th and 1583rd scan-points was compared with the sum of the three T_δ values from the 1585th, the 1584th, and the 1583rd scan-points to screen the next scan-point of the 1583rd. To calibrate the intensities of the 1584th and 1585th scan-points, the blue calibrated line based on the intensities of the 1586th and 1583rd scan-points and shown in Fig. 3(B) was used. The calculated intensities of 5287.4 counts for the 1584th scan-point and 6974.9 counts for the 1585th scan-point were obtained as shown in Fig. 3(B′). Second, the stop-point always occurs when its intensity is below 500 counts or when its S/N is more than 3. If the last scan-point is the suspicious scan-point, the previous scan-point is defined as the stop-point. For example, the 1580th and 1596th scan-points were the stop-points in Fig. 3(B). However, if the last several scan-points are consecutive suspicious scan-points, the CPR algorithm may not be applicable for this ion since the deletion of several scan-points can result in an incomplete EIC peak. In addition, the choice of the T_δ value for each calculated δ value is dependent on the lower intensity of adjacent scan-points. The scan-sorted MS peak tables of pyrimethanil and ethoprophos before and after reconstruction can be seen in Supplementary Tables S1–S4 (see Supporting Information).

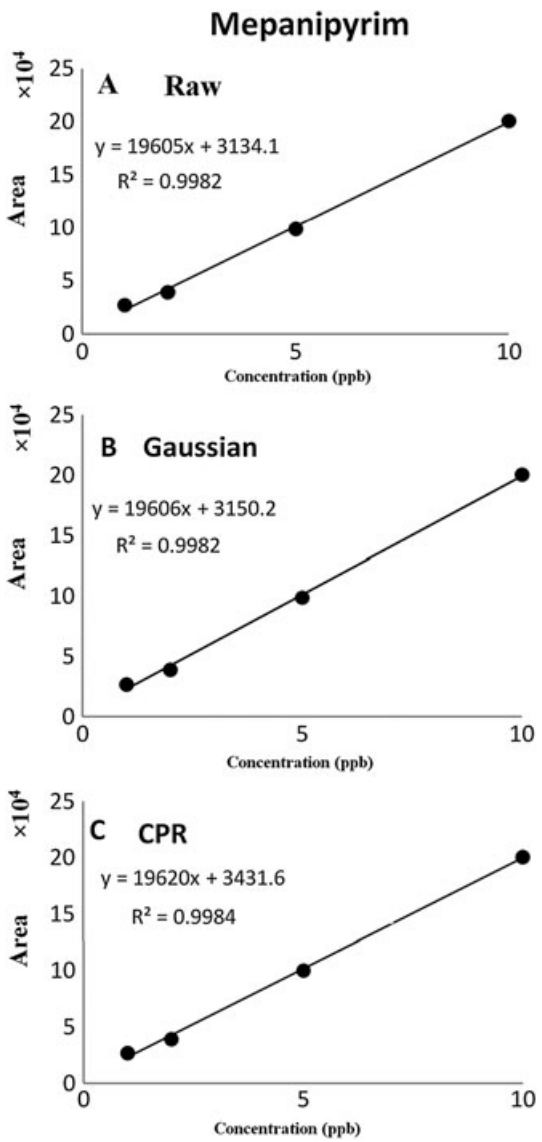

Figure 4. Equations and correlation coefficients of raw, Gaussian and reconstructed calibration curves for mepanipyrim.

Table 1. Structural confirmation of pre-CPR and post-CPR

Pesticide	*Q* ion (*m/z*)	*q* ion (*m/z*)	q/Q_{raw} (%)[a]	q/Q_{rec} (%)[b]	q/Q_{ref} (%)[c] with its confidence region
Tetradifon	158.9666	110.9996	72.7	75.7	65.1[58.6–71.6]
Ametryn	227.1199	212.0964	83.9	83.4	76.1[68.5–83.7]
Fipronil	366.9429	350.9480	85.0	83.1	74.3[66.9–81.7]
Trifluralin	264.0227	306.0696	61.3	60.3	55.2[49.7–60.7]
o-Phenylphenol	170.0726	169.0648	104.7	104.4	92.6[83.3–101.9]

[a]The *q*/*Q* value obtained from pre-CPR.
[b]The *q*/*Q* value obtained from post-CPR.
[c]The reference *q*/*Q* value in self-built database.

Rapid Communications in Mass Spectrometry

Investigation of CPR in pesticide residue analysis

The developed CPR method focuses on low-abundance ions or even trace ions. Thus, it possesses great potential in pesticide residue analysis. In our investigation, CPR provided not only structural confirmation, but also quantitative analysis.

Structural confirmation

The developed CPR algorithm was applied to an apple sample spiked with 118 pesticides to evaluate its structural confirmation ability. According to European Council Directive 96/23/EC,[36] at least two representative ions per pesticide are required to ensure its structural confirmation in high-resolution MS screening. The response ratio *q/Q* (*q*: the qualitative ion; *Q*: the quantitative ion) of the two representative ions should be within a specified tolerance. Adhering to this directive, our accurate, self-built mass database was used to match the experimental ratios. The application of CPR was attempted to discover the suspicious scan-points in the EIC peaks and to modify the corresponding response ratios. In the process, the peak area of each target ion was calibrated based on the reconstructed EIC peak. Thus, the response ratio was re-calculated and compared with the reference from the database.

A total of 107 pesticides met the directive and their reconstructed *q/Q* values were kept within the specified tolerances. As an example, in Table 1, the pre-CPR *q/Q* value of ametryn (*q*: *m/z* 212.0964, *Q*: *m/z* 227.1199) was calculated to be 83.9, which exceeded the confidence region of its reference and led to a negative conformation. After correction using the CPR algorithm, the EIC peaks at *m/z* 227.1199 and 212.0964 were reconstructed, and the *q/Q* value was re-calculated to be 83.4. The improvement in the EIC shape decreased the deviation of the *q/Q* value and contributed to ametryn being confirmed at a lower residual level in the complex matrix. Yet, there were still 11 pesticides that could not be confirmed, even after correction using the CPR algorithm and subsequent re-calculation. Of these, eight pesticides had signals of their representative ions that were too low to perform the CPR, and the other three showed corrected *q/Q* values that remained outside the confidence level (Table 1). Still, it was encouraging to note that the post-CPR *q/Q* values of two of the three pesticides became closer to their references, which showed a certain degree of positive effect of CPR on enhancing structural confirmation.

Quantitative analysis

To evaluate the performance of the CPR algorithm in quantitative analysis, 10 pesticides throughout the GC/MS cycle were selected randomly from the 107 test pesticides. The raw calibration curves (Fig. 4(A)) were built by detecting apple samples spiked with standard pesticides at 1, 2, 5, and 10 ppb. Instead of the raw peak, the Gaussian peak was generated by smoothing the raw EIC peak of each pesticide at 5 ppb (the Gaussian algorithm is a frequently used smoothing method for EIC peaks) to build a new calibration curve (Fig. 4(B)). Furthermore, the EIC peak of each pesticide at 5 ppb was reconstructed with CPR, and the new calibration curve thus built can be seen in Fig. 4(C). The correlation coefficients (R^2) of the calibration curves after the smoothing or the reconstruction were still greater than 0.9900. This illustrated that the slight calibrations of the smoothing or the reconstruction would not cause a large change to the whole calibration curve.

The quantitative results for the 10 test pesticides at 5 ppb after smoothing and reconstruction can be seen in Table 2. The raw and Gaussian relative errors were ±2.29% and ±2.23%, respectively. The slight change in the Gaussian results had little advantage in the quantitative analysis since this algorithm adjusted the EIC peak with only the consideration of achieving a perfect peak pattern. Compared with the Gaussian algorithm, the CPR in this paper purposefully calibrated the intensities of the suspicious scan-points to obtain a more accurate area of the target EIC peak. The reconstructed relative errors were less than ±1.55% and the reconstructed

Table 2. Quantitative results of raw, Gaussian and reconstructed EIC peaks

	Quantitative result[a]					
Pesticide	C_{raw}[b]	Relative error (%)	C_{gau}[c]	Relative error (%)	C_{rec}[d]	Relative error (%)
Pyrimethanil	4.93	−1.42	4.93	−1.42	4.93	−1.38
Tolclofos-methyl	4.96	−0.84	4.95	−0.91	4.94	−1.23
Mepanipyrim	4.89	−2.29	4.89	−2.23	4.94	−1.18
delta-BHC	5.01	0.16	5.02	0.37	5.07	1.48
Prometryn	4.89	−2.18	4.90	−1.96	4.94	−1.18
Quinalphos	5.00	−0.05	5.03	0.51	5.02	0.43
Prothiofos	5.07	1.33	5.07	1.40	5.03	0.53
o,p'-Methoxychlor	5.06	1.16	5.06	1.18	5.03	0.57
Octicizer	4.94	−1.17	4.93	−1.38	4.96	−0.75
Tebufenpyrad	4.94	−1.17	4.93	−1.48	4.92	−1.55
Extremum of relative error (%)		−2.29		−2.23		−1.55
SD	0.06		0.07		0.05	

[a]The prepared concentration of ten pesticides was 5 ppb.
[b]The calculated concentration of raw EIC peaks.
[c]The calculated concentration of Gaussian EIC peaks.
[d]The calculated concentration of reconstructed EIC peaks.

standard deviation (SD) of 10 test pesticides also decreased. The better quantitative result of the reconstruction further showed that interference in the reconstructed EIC peaks was reduced. Even so, the reconstructed results of tolclofos-methyl, delta-BHC, quinalphos, and tebufenpyrad showed some negative aspects of the CPR algorithm since incorrect assignment may have been made. However, their reconstructed EIC peak still can be used for accurate quantitative analysis because the relative errors were kept small. Comparing the Gaussian algorithm with the CPR algorithm, we can find that the effect of the CPR is more obvious and positive for the pesticides that have larger relative errors. This reflects the capacity of CPR to reduce interfering signals and the impact of interfering signals on true signals. On the other hand, the CPR is reliable and would not cause a distortion of the analytical results since this algorithm only modifies the suspicious scan-points in the target EIC peak instead of removing them.

CONCLUSIONS

For an ion with low abundance, the relative deviation between adjacent scanned *m/z* values was found inversely proportional to the MS peak intensity. It provided a way to improve the trace analysis. Therefore, a CPR algorithm was developed for processing the recorded data from GC/TOFMS. Briefly, the CPR algorithm included the estimation of thresholds for relative deviations, the screening of suspicious scan-points in target EIC peaks, and the reconstruction of new EIC peaks.

When CPR was employed in the analysis of trace pesticide residue, the reconstructed EIC peak decreased the impact of interference on the peak areas and the *q/Q* values. It contributed to analytes being confirmed and quantified at a lower residual level. In the current evaluation study, 107 out of 118 test pesticides at 5 ppb were confirmed successfully and the corrected *q/Q* values became closer to their references. In quantification, compared with the prepared concentration of 5 ppb, the relative errors of the calculated concentrations of 10 test pesticides were all below ±1.55%. Although the result improved slightly, it demonstrated that the CPR algorithm could be used as an independent or auxiliary method for the qualification and quantification, especially in the cases of trace analytes. From another point of view, the slight change in the results also indicated the reliability of the CPR algorithm because the CPR does not cause the distortion of the raw results. Thus, the developed CPR algorithm will be helpful in the analysis of trace pesticide residues in complex matrices.

Acknowledgement

This study was supported by the National Natural Science Foundation of China (No. 21402231).

REFERENCES

[1] T. Cai, L. Zhang, H. Wang, J. Zhang, Y. Guo. Assisted inhibition effect of acetylcholinesterase with n-octylphosphonic acid and application in high sensitive detection of organophosphorous pesticides by matrix-assisted laser desorption/ionization Fourier transform mass spectrometry. *Anal. Chim. Acta* **2011**, *706*, 291.
[2] S. Coelho. European pesticide rules promote resistance, researchers warn. *Science* **2009**, *323*, 450.
[3] R. Fan, F. Zhang, H. Wang, L. Zhang, J. Zhang, Y. Zhang, C. Yu, Y. Guo. Reliable screening of pesticide residues in maternal and umbilical cord sera by gas chromatography-quadrupole time of flight mass spectrometry. *Sci. Chin. Chem.* **2014**, *57*, 669.
[4] Z. H. Rivera, E. Oosterink, L. Rietveld, F. Schoutsen, L. Stolker. Influence of natural organic matter on the screening of pharmaceuticals in water by using liquid chromatography with full scan mass spectrometry. *Anal. Chim. Acta* **2011**, *700*, 114.
[5] J. F. García-Reyes, B. Gilbert-López, A. Molina-Díaz, A. R. Fernández-Alba. Determination of pesticide residues in fruit-based soft drinks. *Anal. Chem.* **2008**, *80*, 8966.
[6] F. Zhang, C. Yu, W. Wang, R. Fan, Z. Zhang, Y. Guo. Rapid simultaneous screening and identification of multiple pesticide residues in vegetables. *Anal. Chim. Acta* **2012**, *757*, 39.
[7] S. Walorczyk. Application of gas chromatography/tandem quadrupole mass spectrometry to the multi-residue analysis of pesticides in green leafy vegetables. *Rapid Commun. Mass Spectrom.* **2008**, *22*, 3791.
[8] M. I. Cervera, C. Medina, T. Portolés, E. Pitarch, J. Beltrán, E. Serrahima, L. Pineda, G. Muñoz, F. Centrich, F. Hernández. Multi-residue determination of 130 multiclass pesticides in fruits and vegetables by gas chromatography coupled to triple quadrupole tandem mass spectrometry. *Anal. Bioanal. Chem.* **2010**, *397*, 2873.
[9] A. G. Frenich, M. J. González-Rodríguez, F. J. Arrebola, J. L. Martínez Vidal. Potentiality of gas chromatography-triple quadrupole mass spectrometry in vanguard and rearguard methods of pesticide residues in vegetables. *Anal. Chem.* **2005**, *77*, 4640.
[10] Z. Wang, Q. Chang, J. Kang, Y. Cao, N. Ge, C. Fan, G.-F. Pang. Screening and identification strategy for 317 pesticides in fruits and vegetables by liquid chromatography-quadrupole time-of-flight high resolution mass spectrometry. *Anal. Methods* **2015**, *7*, 6385.
[11] F. Hernández, M. I. Cervera, T. Portolés, J. Beltrán, E. Pitarch. The role of GC–MS/MS with triple quadrupole in pesticide residue analysis in food and the environment. *Anal. Methods* **2013**, *5*, 5875.
[12] S. Grimalt, Ó. J. Pozo, J. V. Sancho, F. Hernández. Use of liquid chromatography coupled to quadrupole time-of-flight mass spectrometry to investigate pesticide residues in fruits. *Anal. Chem.* **2007**, *79*, 2833.
[13] A. Uclés Moreno, S. Herrera López, B. Reichert, A. Lozano Fernández, M. D. Hernando Guil, A. R. Fernández-Alba. Microflow liquid chromatography coupled to mass spectrometry – An approach to significantly increase sensitivity, decrease matrix effects, and reduce organic solvent usage in pesticide residue analysis. *Anal. Chem.* **2015**, *87*, 1018.
[14] T. Portolés, J. G. J. Mol, J. V. Sancho, F. J. López, F. Hernández. Validation of a qualitative screening method for pesticides in fruits and vegetables by gas chromatography quadrupole-time of flight mass spectrometry with atmospheric pressure chemical ionization. *Anal. Chim. Acta* **2014**, *838*, 76.
[15] F. Zhang, H. Wang, L. Zhang, J. Zhang, R. Fan, C. Yu, W. Wang, Y. Guo. Suspected-target pesticide screening using gas chromatography-quadrupole time-of-flight mass spectrometry with high resolution deconvolution and retention index/mass spectrum library. *Talanta* **2014**, *128*, 156.
[16] F. Hernández, T. Portolés, E. Pitarch, F. J. López. Target and nontarget screening of organic micropollutants in water by solid-phase microextraction combined with gas chromatography/high-resolution time-of-flight mass spectrometry. *Anal. Chem.* **2007**, *79*, 9494.

[17] T. Portolés, J. V. Sancho, F. Hernández, A. Newton, P. Hancock. Potential of atmospheric pressure chemical ionization source in GC-QTOF MS for pesticide residue analysis. *J. Mass Spectrom.* **2010**, *45*, 926.
[18] L. Vergeynst, H. Van Langenhove, P. Joos, K. Demeestere. Accurate mass determination, quantification and determination of detection limits in liquid chromatography-high-resolution time-of-flight mass spectrometry: challenges and practical solutions. *Anal. Chim. Acta* **2013**, *789*, 74.
[19] L. Cherta, T. Portolés, E. Pitarch, J. Beltran, F. J. López, C. Calatayud, B. Company, F. Hernández. Analytical strategy based on the combination of gas chromatography coupled to time-of-flight and hybrid quadrupole time-of-flight mass analyzers for non-target analysis in food packaging. *Food Chem.* **2015**, *188*, 301.
[20] V. V. Mihaleva, O. Vorst, C. Maliepaard, H. A. Verhoeven, R. C. H. de Vos, R. D. Hall, R. C. H. J. van Ham. Accurate mass error correction in liquid chromatography time-of-flight mass spectrometry based metabolomics. *Metabolomics* **2008**, *4*, 171.
[21] L. Miao, W. Cai, X. Shao. Rapid analysis of multicomponent pesticide mixture by GC–MS with the aid of chemometric resolution. *Talanta* **2011**, *83*, 1247.
[22] Z. Liu, W. Cai, X. Shao. High-throughput approach for analysis of multicomponent gas chromatographic-mass spectrometric signals. *J. Chromatogr. A* **2009**, *1216*, 1469.
[23] B. O. Keller, J. Suj, A. B. Young, R. M. Whittal. Interferences and contaminants encountered in modern mass spectrometry. *Anal. Chim. Acta* **2008**, *627*, 71.
[24] W. Windig, J. M. Phalp, A. W. Payne. A noise and background reduction method for component detection in liquid chromatography mass spectrometry. *Anal. Chem.* **1996**, *68*, 3602.
[25] Y. Li, H. Qu, Y. Cheng. An entropy-based method for noise reduction of liquid chromatography-mass spectrometry data. *Anal. Chim. Acta* **2008**, *612*, 19.
[26] W. Windig. The use of the Durbin-Watson criterion for noise and background reduction of complex liquid chromatography/mass spectrometry data and a new algorithm to determine sample differences. *Chemom. Intell. Lab. Syst.* **2005**, *77*, 206.
[27] H. Zhang, M. Grubb, W. Wu, J. Josephs, W. G. Humphreys. Algorithm for thorough background subtraction of high-resolution LC/MS data: Application to obtain clean product ion spectra from nonselective collision-induced dissociation experiments. *Anal. Chem.* **2009**, *81*, 2695.
[28] H. Zhang, L. Petrone, J. Kozlosky, L. Tomlinson, G. Cosma, J. Horvath. Pooled sample strategy in conjunction with high-resolution liquid chromatography-mass spectrometry-based background subtraction to identify toxicological markers in dogs treated with ibipinabant. *Anal. Chem.* **2010**, *82*, 3834.
[29] G. Yan, A. Zhang, H. Sun, Y. Han, H. Shi, Y. Zhou, X. Wang. An effective method for determining the ingredients of Shuanghuanglian formula in blood samples using high-resolution LC–MS coupled with background subtraction and a multiple data processing approach. *J. Sep. Sci.* **2013**, *36*, 3191.
[30] P. Zhu, W. Ding, W. Tong, A. Ghosal, K. Alton, S. Chowdhury. A retention-time-shift-tolerant background subtraction and noise reduction algorithm (BgS-NoRA) for extraction of drug metabolites in liquid chromatography/mass spectrometry data from biological matrices. *Rapid Commun. Mass Spectrom.* **2009**, *23*, 1563.
[31] H. Zhang, Y. Yang. An algorithm for thorough background subtraction from high-resolution LC/MS data: application for detection of glutathione-trapped reactive metabolites. *J. Mass Spectrom.* **2008**, *43*, 1181.
[32] S.-Y. Wang, C.-H. Kuo, Y. J. Tseng. Ion trace detection algorithm to extract pure ion chromatograms to improve untargeted peak detection quality for liquid chromatography/time-of-flight mass spectrometry-based metabolomics data. *Anal. Chem.* **2015**, *87*, 3048.
[33] L. A. Adutwum, J. J. Harynuk. Unique ion filter: a data reduction tool for GC/MS data preprocessing prior to chemometric analysis. *Anal. Chem.* **2014**, *86*, 7726.
[34] T. -J. Ho, C. -H. Kuo, S. -Y. Wang, G. -Y. Chen, Y. J. Tseng. True ion pick (TIPick): a denoising and peak picking algorithm to extract ion signals from liquid chromatography/mass spectrometry data. *J. Mass Spectrom.* **2013**, *48*, 234.
[35] A. V. Tolmachev, M. E. Monroe, N. Jaitly, V. A. Petyuk, J. N. Adkins, R. D. Smith. Mass measurement accuracy in analyses of highly complex mixtures based upon multidimensional recalibration. *Anal. Chem.* **2006**, *78*, 8374.
[36] European Commission Decision. Concerning the performance of analytical methods and the interpretation of results. Document No. L221, Implementing Council Directive 96/23/EC.

SUPPORTING INFORMATION

Additional supporting information may be found in the online version of this article at the publisher's website.

